Semimajor Axis Estimation Strategies

Jonathan P. How[*]

MIT Department of Aeronautics and Astronautics

Kyle T. Alfriend [†]

Texas A&M Department of Aerospace Engineering

Louis Breger[‡] and Megan Mitchell[§]

MIT Department of Aeronautics and Astronautics

This paper extends previous analysis on the impact of sensing noise for the navigation and control aspects of formation flying spacecraft. We analyze the use of Carrier-phase Differential GPS (CDGPS) in relative navigation filters, with a particular focus on the filter correlation coefficient. This work was motivated by previous publications which suggested that a "good" navigation filter would have a strong correlation (i.e., coefficient near -1) to reduce the semimajor axis (SMA) error, and therefore, the overall fuel use. However, practical experience with CDGPS-based filters has shown this strong correlation seldom occurs (typical correlations ≈ -0.1), even when the estimation accuracies are very good. We derive an analytic estimate of the filter correlation coefficient and demonstrate that, for the process and sensor noises levels expected with CDGPS, the expected value will be very low. It is also demonstrated that this correlation can be improved by increasing the time step of the discrete Kalman filter, but since the *balance* condition is not satisfied, the SMA error also increases. These observations are verified with several linear simulations. The combination of these simulations and analysis provide new insights on the crucial role of the process noise in determining the semimajor axis knowledge.

I.   Introduction

In formation flying missions, accurate knowledge of the difference in semimajor axes, or equivalently, the difference in orbital energy, between the vehicles in the formation is important.[4,6,7] A difference in semimajor axes means that the two vehicles have different orbital periods and thus they will drift out of formation unless considerable control effort is applied.[3] The output of the CDGPS Kalman filter includes the relative formation state in a Local Vertical Local Horizontal (LVLH) reference frame. Understanding the relationship between position and velocity accuracies and semimajor axis accuracy is key to evaluating the output of this type of filter. While Ref. [4] develops the navigation error analysis from absolute state relations, the results can be reformulated for the relative case. Ref. [5] analyzed that case in detail, comparing linear and nonlinear simulation results with analytic predictions. This paper extends the previous work to consider further modifications to the Carrier-Phase Differential GPS (CDGPS) Kalman filter to determine their effect on the *correlation* and *balance*, which are the two key properties. This includes further details on the analytic predictions, an analysis of the effect of adding velocity sensing, and an investigation of the impact of increasing the time step in the discrete Kalman filter.

The relative navigation error equations, shown below, relate semimajor axis error to position and velocity errors. Note that this discussion is limited to circular reference orbits. The standard deviation of the

---

[*]Associate Professor, MIT Department of Aeronautics and Astronautics, jhow@mit.edu

[†]Professor, Texas A&M Department of Aerospace Engineering, alfriend@aero.tamu.edu

[‡]Research Assistant, MIT Department of Aeronautics and Astronautics, lbreger@mit.edu

[§]MIT Department of Aeronautics and Astronautics, meganleigh@gmail.com
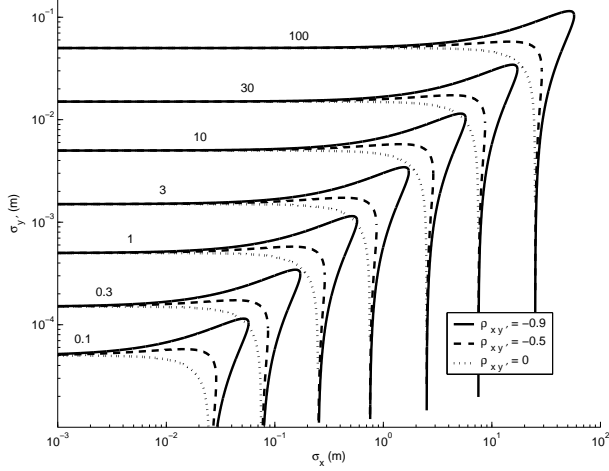
Fig. 1: Contours of constant semimajor axis vs. position and velocity accuracy. Contours given for 3 levels of correlation.
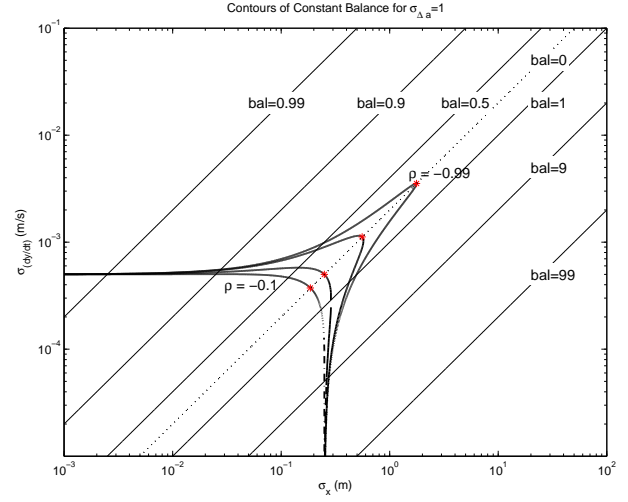
Fig. 2: Contours of constant balance (straight lines) illustrate region where correlation affects SMA accuracy. Numbers indicate balance index.

differential semimajor axis estimate, $\sigma_{\Delta a}$, is given by[4]

$$\sigma_{\Delta a} = 2\sqrt{4\sigma_x^2 + \frac{4}{n}\rho_{x\dot{y}}\sigma_x\sigma_{\dot{y}} + \frac{1}{n^2}\sigma_{\dot{y}}^2} \tag{1}$$

The parameters σ_x, $\sigma_{\dot{y}}$, and $\rho_{x\dot{y}}$ are derived from the error covariance matrix for the relative LVLH state estimate, $\hat{\mathbf{x}} = [\begin{array}{cccc} x & y & \dot{x} & \dot{y} \end{array}]^T$ with estimation error $\tilde{\mathbf{x}} = \hat{\mathbf{x}} - \mathbf{x}$, which is assumed to be unbiased, $E[\tilde{\mathbf{x}}] = \mathbf{0}$, and have a covariance

$$E[\tilde{\mathbf{x}}\tilde{\mathbf{x}}^T] = \begin{bmatrix} \sigma_x^2 & \rho_{xy}\sigma_x\sigma_y & \rho_{x\dot{x}}\sigma_x\sigma_{\dot{x}} & \rho_{x\dot{y}}\sigma_x\sigma_{\dot{y}} \\ \rho_{yx}\sigma_y\sigma_x & \sigma_y^2 & \rho_{y\dot{x}}\sigma_y\sigma_{\dot{x}} & \rho_{y\dot{y}}\sigma_y\sigma_{\dot{y}} \\ \rho_{\dot{x}x}\sigma_{\dot{x}}\sigma_x & \rho_{\dot{x}y}\sigma_{\dot{x}}\sigma_y & \sigma_{\dot{x}}^2 & \rho_{\dot{x}\dot{y}}\sigma_{\dot{x}}\sigma_{\dot{y}} \\ \rho_{\dot{y}x}\sigma_{\dot{y}}\sigma_x & \rho_{\dot{y}y}\sigma_{\dot{y}}\sigma_y & \rho_{\dot{y}\dot{x}}\sigma_{\dot{y}}\sigma_{\dot{x}} & \sigma_{\dot{y}}^2 \end{bmatrix} \tag{2}$$

Note that if the radial position and in-track velocity are linearly correlated ($\rho_{x\dot{y}} = -1$), the expression for semimajor axis variance from Eq. 1 reduces to

$$\sigma_{\Delta a} = 2\sqrt{4\sigma_x^2 - \frac{4}{n}\sigma_x\sigma_{\dot{y}} + \frac{1}{n^2}\sigma_{\dot{y}}^2} = 2\sqrt{\left(2\sigma_x^2 - \frac{1}{n}\sigma_{\dot{y}}\right)^2} \tag{3}$$

If the position and velocity error are linearly correlated <u>and</u> satisfy

$$\sigma_{\dot{y}} = 2n\sigma_x \tag{4}$$

then the position and velocity errors cancel and there is **no** error in the semimajor axis estimate. In other words, the two requirements for zero semimajor axis variance are:

$$\rho_{x\dot{y}} = -1 \quad \text{and} \quad \sigma_{\dot{y}} = 2n\sigma_x$$

which will subsequently be referred to as the correlation and balance requirements.

The relationship between σ_x, $\sigma_{\dot{y}}$, $\rho_{x\dot{y}}$, and $\sigma_{\Delta a}$ is illustrated in Fig. 1.[4] The x and y axes of the plot are the standard deviations of the position and velocity estimation errors. Contours of constant semimajor axis standard deviation are shown on the figure. Each contour is associated with a value of $\rho_{x\dot{y}}$ in addition to a level of $\sigma_{\Delta a}$; several values of $\rho_{x\dot{y}}$ are shown for each level of $\sigma_{\Delta a}$. The diagonal of peaks indicates where $\sigma_{\dot{y}} = 2n\sigma_x$. Along the diagonal of peaks, the lines of constant semimajor axis experience a "bump"

2nd International Symposium on Formation Flying Missions & Technologies
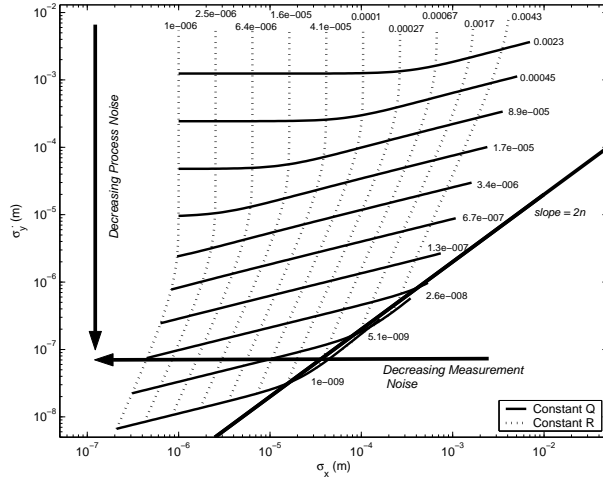
Fig. 3: Contours of constant Q and R are shown on axes of position and velocity accuracy.
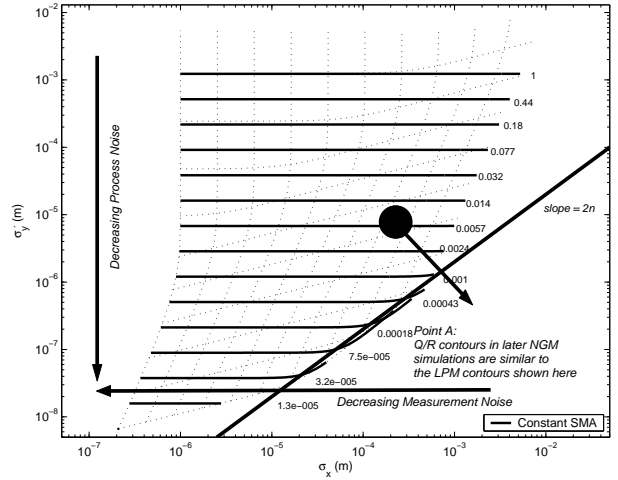
Fig. 4: Contours of constant semimajor axis shown vs position/velocity accuracy. Contours of constant Q and R are dotted lines in background.

that increases in size as the correlation tends towards -1. This bump corresponds to increasing cancelation between the error in x and $\dot{y}$ that results from increasing correlation in these errors. Essentially, if the errors have high correlation and the proper balance, the higher error levels can be tolerated with the same resulting semimajor axis error. Each point on the graph corresponds to a unique set of σ_x and $\sigma_{\dot{y}}$. However, many points on the graph are intersected by more than one contour of constant semimajor axis. It is the correlation that determines the specific contour on which the system lies. Fig. 2 shows the contours for a constant value of the semimajor axis error for varying values of correlation. The plot also shows lines of constant *balance index*, which is calculated as

$$\texttt{bal} = \left| 1 - \frac{2n\sigma_x}{\sigma_{\dot{y}}} \right| \tag{5}$$

Clearly $\texttt{bal}$ should be zero when the balance requirement is met. However, the figure shows that if the balance is slightly off, *i.e.,* $\texttt{bal} \approx 0.5$ or $\texttt{bal} \approx |-1|$, then the effects of the correlation are reduced.

II.   Linear Planar Model Simulations with Q and R

This section investigates the relationship between the Kalman filter parameters and the resulting estimate accuracy. These results are based on the premise that the Kalman filter produces the best answer from the given the models and measurements, and that the balance or correlation between elements of the state vector estimate are not important. Initial investigations showed that, predictably, the levels of measurement and process noise have the most influence of the estimate accuracy. These levels are indicators of how well the sensors and the dynamics are modeled. The relative levels of these noises determines how the filter will weigh new measurement information against the current state estimate propagated from the dynamics information. A CDGPS navigation filter has nonlinearities in both the system dynamics and the measurement equations, and because the set of visible GPS satellites changes, the measurement matrix H will change, and the state vector length will grow or shrink as the set of estimated carrier biases changes.[12] These factors make it difficult to understand direct relationships between the filter parameters and the navigational accuracies. Thus, we started with a simplified Linear Planar Model (LPM) to develop insights into the behavior of a relative navigation filter using CDGPS.[5]

Meeting the balance and correlation requirements discussed in Section I corresponds to being on the "bump" in Fig. 1, but the baseline results of the LPM simulation were above this region. This leads to the question of how changing filter inputs will move the output closer to or further from the bump. To answer this question, the LPM simulation was run for a range of measurement and process noise levels.

For each unique assignment of Q and R, the resulting error variances for radial position and in-track velocity, σ_x and $\sigma_{\dot{y}}$, were recorded. The corresponding semimajor axis error, $\sigma_{\Delta a}$, was calculated using Eq. 1. Fig. 3 shows lines of constant Q and R on axes of σ_x and $\sigma_{\dot{y}}$. The diagonal of peaks on this graph

2nd International Symposium on Formation Flying Missions & Technologies

indicates the location of the "bump," where the balance and correlation requirements are met (which means $\sigma_{\dot{y}} = 2n\sigma_x$). By moving from one line of constant Q or R to another, one can see how decreasing the process or measurement noise would change the resulting position and velocity error. However, it is semimajor axis knowledge, not just position and velocity knowledge, that is important for control performance.

Several graphs demonstrate the relationship between Q, R and $\sigma_{\Delta a}$. First, Fig. 4 is reproduced and lines of constant semimajor axis error added. The lines for constant Q and R are dimmed for clarity. Note the lines of constant semimajor axis are horizontal, which corresponds with the horizontal sections of the semimajor axis contours on Fig. 1. The effect of changes in Q and R on $\sigma_{\Delta a}$ can be assessed by looking at the constant lines for all three values. Because the lines of constant semimajor axis are horizontal, improvement in $\sigma_{\Delta a}$ can only be accomplished by moving in the vertical direction on the graph, which is equivalent to decreasing $\sigma_{\dot{y}}$. Whether this requires decreasing Q or R depends on the angles between the horizontal lines of constant $\sigma_{\Delta a}$ and the contours of constant Q and R.
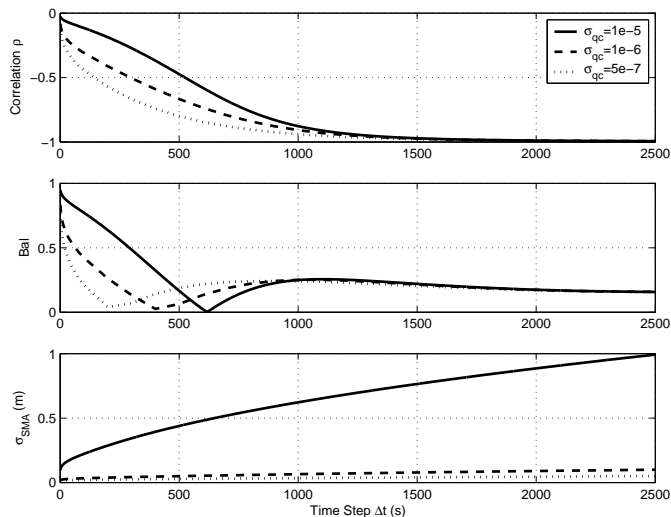
The LPM results shown thus far occupy the region above the $\sigma_{\dot{y}} = 2n\sigma_x$ line. Ref. [5] investigated three questions about the system: (i) What features of the system cause this behavior? (ii) Does this agree with expected behavior? (iii) What is required to cause the LPM results to move closer to this line, and below the line?

This was done by modifying the LPM to put more emphasis on the orbital dynamics in the Kalman filter. This was based on the observation that it is reasonable to expect the correlation between radial position and in-track velocity will increase only when the estimate depends more on the dynamics model embedded in the filter. The following extends the previous analysis to consider the effects of other changes to the Kalman Filter and to expand the analytic results.

III.   Discrete Simulations for Varying Δt

One way to put more emphasis on the dynamics model is to reduce the measurement rate. Prior analysis of the CDGPS filter by Busse[12] used a 1 Hz rate, although much longer time steps were considered in Ref. [11]. One difficulty with increasing the propagation time is that the nonlinearity in the orbit propagation becomes much more significant, and more sophisticated models and propagation algorithms must be used, especially for the error covariance.[14,15] The following investigation of the effect of varying measurement update rate by changing the discretization time step uses the linear model and thus ignores these effects.

To do this, a family of discrete Riccati equations was solved using Hill's dynamics at various discretization times. In each case, the constant spectral density matrix Q_c associated with the process noise of the continuous dynamics was converted to the appropriate discrete process

Fig. 5: Filter correlation, balance, and SMA error for various discretization time steps Δt (seconds).

noise Q_d using the conversion algorithm in Ref. [13] (`DISRW` in Chapter 9). The simulation results in Figure 5 were done for several values of $\sigma_{qc} = \{10^{-5}, 10^{-6}, 5 \times 10^{-7}\}m/s^{3/2}$ ($Q_c = \sigma_{qc}^2 I_2$) and a constant sensing noise covariance $R = (5 \times 10^{-3}\text{m})^2$. The plots shows that, as the discretization time step is increased, the correlation coefficient tends to -1. This trend is expected, because longer propagation times will force increased filter dependence on the equations of motion, translating into increased overall correlation[a]. However, the proper position to velocity error balance is not achieved, causing the SMA accuracy to degrade. The plot clearly shows the role of the process noise Q_c in determining the SMA error growth.

---

[a]One caution: the correlation approaches -1 for filter time steps larger than 1000 seconds for which the nonlinearity in the dynamics will play an important role.

Comparing this result to Fig. 2, it can be seen that while the balance index is not zero, it is producing the effect of lowering the overall semimajor axis in combination with the correlation. However, the canceling effects of correlation and balance are not sufficient to prevent the semimajor axis error from growing rapidly as the time step is increased. Thus, decreasing the measurement update rate to produce higher correlation is not a viable strategy for reducing semimajor axis error.

IV.   Agreement with Analytical Work

The analysis in this section develops analytical relationships between the process and measurement noise levels and the errors and correlations. The link between the two is established through the algebraic Riccati equation. The matrix Riccati equation has no known analytic solution for system more complicated than a double integrator. However, for a Kalman filter with a time step $\Delta t \approx 1$ second for a 90 minute orbit, the coupling between motion in the x and y directions is very weak and the dynamics can be well approximated as two weakly coupled double integrators.

Start with the planar equations of motion in an LVLH frame about a circular reference orbit with frequency n

$$\ddot{x} - 2n\dot{y} - 3n^2 x = f_x \tag{6}$$
$$\ddot{y} + 2n\dot{x} = f_y \tag{7}$$

where f_x and f_y are disturbance accelerations with identical spectral densities σ_Q^2. We can write this in state space form using $X = [x, \dot{x}, y, \dot{y}]^T$ and dynamics matrices A_h and B_h. When only position measurements are available, the output matrix is

$$H_h = \begin{bmatrix} 1 & 0 & 0 & 0 \\ 0 & 0 & 1 & 0 \end{bmatrix} \tag{8}$$

with sensing noise given by σ_R^2 on each measurement. These dynamics can be transformed to a new system of equations with the state $\bar{X} = [x, x', y, y']^T$, where $(*)' = (\dot{*})\Delta t$, $\bar{X} = T_p X$, and $T_p = \text{diag}([\ 1 \quad \Delta t \quad 1 \quad \Delta t\ ])$, to yield

$$x'' = 2\epsilon y' + 3\epsilon^2 x + (\Delta t)^2 f_x \tag{9}$$
$$y'' = -2\epsilon x' + (\Delta t)^2 f_y \tag{10}$$

with $\epsilon = n\Delta t$. Note that when $\epsilon \ll 1$, which is true for this application, the x and y dynamics can essentially be written as double integrators for which the solution of the Riccati equation is easily found. The combined dynamics then consist of these two double integrators with coupling terms of order ϵ and ϵ^2.

A.   Correlation with Position Measurements

The dynamics in Eqs. 9 and 10 are written in state space form as

$$\bar{X}' = \bar{A}\bar{X} + \bar{B}f \tag{11}$$

where $\bar{A} = \Delta t(T_P A_h T_P^{-1})$, $\bar{B} = \Delta t(T_p B_h)$, and $\bar{H} = H_h$. The differential filter Riccati equation for the original system (Eqs. 6 and 7) must also be transformed using T_p, and the result is that, at steady state

$$\mathbf{0} = \bar{A}P + P\bar{A}^T + \bar{B}Q\bar{B}^T - P\bar{H}^T R^{-1}\bar{H}P \tag{12}$$

where $Q = (\sigma_Q^2/\Delta t)I_2$ and $R = (\sigma_R^2/\Delta t)I_2$, with the factors of $1/\Delta t$ resulting from the transformation. To proceed, the covariance for the transformed state is represented as a Taylor expansion in ϵ. Substituting the expressions for $P = P_0 + \epsilon P_1 + \epsilon^2 P_2$ and $\bar{A} = A_0 + \epsilon A_1 + \epsilon^2 A_2$ in the Riccati equation and grouping terms in the same power of ϵ, it is possible to solve for the expansion of the covariance matrix (P_{kxx}, $P_{ky'y'}$, and $P_{kxy'}$, $k = 0, 1, 2$). The $\bar{A}$ matrix in Eq. 11 gives the expansion matrices A_0 and A_1

$$A_0 = \begin{bmatrix} A_{00} & 0_2 \\ 0_2 & A_{00} \end{bmatrix} \qquad A_1 = \begin{bmatrix} 0_2 & A_{11} \\ -A_{11} & 0_2 \end{bmatrix} \tag{13}$$

$$A_{00} = \begin{bmatrix} 0 & 1 \\ 0 & 0 \end{bmatrix} \qquad A_{11} = \begin{bmatrix} 0 & 0 \\ 0 & 2 \end{bmatrix} \tag{14}$$

Define $\mathbf{x} = [\ x \quad x'\ ]^T$ and $\mathbf{y} = [\ y \quad y'\ ]^T$. Then $P_{0\mathbf{xy}} = \mathbf{0}$ for the solution of the two independent double integrators. The first-order solution to the Riccati equation is computed using

$$A = \begin{bmatrix} 0 & 1 \\ 0 & 0 \end{bmatrix} \qquad\qquad B = \begin{bmatrix} 0 \\ \Delta t^2 \end{bmatrix} \qquad\qquad H = [\ 1 \quad 0\ ] \tag{15}$$

and is found to be

$$P_{0\mathbf{xx}} = P_{0\mathbf{yy}} = \begin{bmatrix} \sqrt{2}\sigma_Q^{\frac{1}{2}}\sigma_R^{\frac{3}{2}} & \sigma_Q\sigma_R\Delta t \\ \sigma_Q\sigma_R\Delta t & \sqrt{2}\sigma_Q^{\frac{3}{2}}\sigma_R^{\frac{1}{2}}\Delta t^2 \end{bmatrix} \tag{16}$$

Substituting into the Riccati equation and isolating $O(\epsilon)$ terms yields

$$P_0 A_1^T + P_1 A_0^T + A_0 P_1 + A_1 P_0 = P_0 D P_1 + P_1 D P_0 \tag{17}$$

$$P_1(A_0^T - DP_0) + (A_0 - P_0 D)P_1 = -(P_0 A_1^T + A_1 P_0) \tag{18}$$

where

$$D = \begin{bmatrix} C & 0_2 \\ 0_2 & C \end{bmatrix} \qquad\qquad C = \frac{\Delta t}{\sigma_R^2}\begin{bmatrix} 1 & 0 \\ 0 & 0 \end{bmatrix} \tag{19}$$

Using knowledge that $P_{0\mathbf{xx}} = P_{0\mathbf{yy}}$,

$$(A_0^T - DP_0) = \begin{bmatrix} E & 0_2 \\ 0_2 & E \end{bmatrix} \tag{20}$$

where

$$E = \begin{bmatrix} -\frac{\Delta t P_{0\mathbf{xx}}}{\sigma_R^2} & -\frac{\Delta t P_{0\mathbf{xx'}}}{\sigma_R^2} \\ 1 & 0 \end{bmatrix} \tag{21}$$

and

$$(A_0 - P_0 D) = \begin{bmatrix} E^T & 0_2 \\ 0_2 & E^T \end{bmatrix} \tag{22}$$

Defining G as

$$G = A_{11}P_{0\mathbf{xx}} - P_{0\mathbf{xx}}A_{11}^T = \begin{bmatrix} 0_2 & -2P_{0\mathbf{xx'}} \\ 2P_{0\mathbf{xx'}} & 0_2 \end{bmatrix} \tag{23}$$

$$\Rightarrow (P_0 A_1^T + A_1 P_0) = \begin{bmatrix} 0_2 & G \\ -G & 0_2 \end{bmatrix} \tag{24}$$

Substituting into the Riccati equation yields

$$\begin{bmatrix} P_{1\mathbf{xx}} & P_{1\mathbf{xy}} \\ P_{1\mathbf{xy}}^T & P_{1\mathbf{yy}} \end{bmatrix}\begin{bmatrix} E & 0_2 \\ 0_2 & E \end{bmatrix} + \begin{bmatrix} E^T & 0_2 \\ 0_2 & E^T \end{bmatrix}\begin{bmatrix} P_{1\mathbf{xx}} & P_{1\mathbf{xy}} \\ P_{1\mathbf{xy}}^T & P_{1\mathbf{yy}} \end{bmatrix} = -\begin{bmatrix} 0_2 & G \\ -G & 0_2 \end{bmatrix} \tag{25}$$

which is a system of three equations

$$P_{1\mathbf{xx}}E + E^T P_{1\mathbf{xx}} = 0_4 \tag{26}$$

$$P_{1\mathbf{yy}}E + E^T P_{1\mathbf{yy}} = 0_4 \tag{27}$$

$$P_{1\mathbf{xy}}E + E^T P_{1\mathbf{xy}} = -G \tag{28}$$

The solution to Eqs. 26 and 27 is $P_{1\mathbf{xx}} = P_{1\mathbf{yy}} = 0$, and Eq. 28 gives

$$P_{1xy'} = -\frac{2\sigma_R^2 P_{0xx'}}{\Delta t P_{0xx}} \qquad P_{1x'y} = -P_{1xy'} \qquad P_{1x'y'} = P_{1xy} = 0 \tag{29}$$

Then the correlation coefficient can be found from

$$\rho_{x\dot{y}} = \frac{P_{x\dot{y}}}{\sqrt{P_{xx}P_{\dot{y}\dot{y}}}} = \frac{P_{xy'}/\Delta t}{\sqrt{P_{xx}P_{y'y'}/\Delta t^2}} \approx \frac{\epsilon P_{1xy'}}{\sqrt{P_{0xx}P_{0y'y'}}} \tag{30}$$

Using the expressions given above, it follows that

$$\rho_{x\dot{y}} \approx -\frac{2(n\Delta t)\sigma_R^2(\sigma_Q\sigma_R\Delta t)}{\sqrt{2}\Delta t\sigma_Q^{\frac{1}{2}}\sigma_R^{\frac{3}{2}}} \left(\sqrt{2}\sigma_Q^{\frac{1}{2}}\sigma_R^{\frac{3}{2}}\sqrt{2}\sigma_Q^{\frac{3}{2}}\sigma_R^{\frac{1}{2}}\Delta t^2\right)^{-1/2} = -\frac{\sqrt{2}\sigma_R^{3-\frac{3}{2}}\sigma_Q^{1-\frac{1}{2}}\Delta t}{\sqrt{2\sigma_Q^2\sigma_R^2\Delta t^2}} \tag{31}$$

$$\approx -n\sqrt{\frac{\sigma_R}{\sigma_Q}} \tag{32}$$

which, upon substitution in Eq. 1, gives a semimajor axis error of

$$\sigma_{\Delta a} = \frac{2^{\frac{5}{4}}}{n}\,\sigma_Q^{\frac{3}{4}}\sigma_R^{\frac{1}{4}} \tag{33}$$

Eqs. 32 and 33 predict the correlation and semimajor axis error variance that can be expected from a continuous Kalman filter. Since these predictions were developed from a model based on two double integrators, the results may not immediately map to the full CDGPS problem. However, these equations agree well with LPM simulations.[5]

To verify the ranges of σ_Q and σ_R for which the equation is valid. The correlation coefficient, $\rho_{x\dot{y}}$, has a limit of -1, so

$$-n\sqrt{\frac{\sigma_R}{\sigma_Q}} \geq -1 \quad \Rightarrow \quad \frac{\sigma_Q}{\sigma_R} \geq n^2 \tag{34}$$

In low Earth orbit ($n \approx 0.001$), Eq. 34 implies that σ_R must be no more than six orders of magnitude larger than σ_Q. Many space-rated GPS receivers produce differential carrier phases measurements with millimeters of error. To achieve $\rho_{x\dot{y}} = -1$, the dynamics environment of the vehicle would have to be modeled to nanometer-level accuracy, which is not currently possible. For a typical example with $\sigma_Q = 1 \times 10^{-6}$ m/s$^{3/2}$ and $\sigma_R = 5 \times 10^{-3}$ ms$^{1/2}$, note that

$$|\rho_{x\dot{y}}| \approx 1 \times 10^{-3}\sqrt{\frac{5 \times 10^{-3}}{1 \times 10^{-6}}} = 0.0707 \ll 1$$

This interpretation of the relationship between correlation and process and measurement noises concurs with conclusions drawn from the LPM examples.

B. Examination of Balance Requirement

One strategy for minimizing the semimajor axis error is to achieve a high correlation and to simultaneously have a balance of errors given by

$$\sigma_{\dot{y}}/\sigma_x = 2n \tag{35}$$

For the transformed state described by Eqs. 9 and 10, this requirement is

$$\sigma_{y'}/\sigma_x = 2n\Delta t \tag{36}$$

Section A showed that for Hill's equations, to first order, the standard deviations for in-track velocity and radial position estimates are

$$\sigma_{y'} \approx \sqrt{P_{0y'y'}} = (\sqrt{2}\sigma_Q^{3/2}\sigma_R^{1/2}\Delta t^2)^{1/2} \tag{37}$$

$$\sigma_x = \sqrt{P_{\mathbf{xx}}} \approx \sqrt{P_{0\mathbf{xx}}} = (\sqrt{2}\sigma_Q^{1/2}\sigma_R^{3/2})^{1/2} \tag{38}$$

Substituting into Eq. 36 gives the analytic expression for the balance condition

$$\sigma_{y'}/\sigma_x = \sqrt{\frac{\sqrt{2}\sigma_Q^{3/2}\sigma_R^{1/2}\Delta t^2}{\sqrt{2}\sigma_Q^{1/2}\sigma_R^{3/2}}} = \Delta t\sqrt{\frac{\sigma_Q}{\sigma_R}} \tag{39}$$

2nd International Symposium on Formation Flying Missions & Technologies

Using Eq. 36, perfect balance requires that

$$\Delta t \sqrt{\frac{\sigma_Q}{\sigma_R}} = 2n\Delta t \quad \Longrightarrow \quad \sqrt{\frac{\sigma_R}{\sigma_Q}} = \frac{1}{2n} \tag{40}$$

This expression can be substituted into Eq. 32 to find the correlation that is achieved when the balance is correct

$$\rho_{x\dot{y}} = -n\sqrt{\frac{\sigma_R}{\sigma_Q}} = -n\left(\frac{1}{2n}\right) = -0.5 \tag{41}$$

This analysis suggests that achieving the required balance in this example is incompatible with achieving a correlation of -1. This indicates that the strategy of minimizing semimajor axis by correlation and balance is impossible.

C.   Correlation with Position and Velocity Measurements

In this example, the system will be augmented with a velocity sensor. The sensor noise and measurement matrices for the transformed double integrator dynamics now take the form

$$R = \begin{bmatrix} \sigma_{rx}^2 & 0 \\ 0 & \sigma_{r\dot{x}}^2 \end{bmatrix} \to \bar{R} = R/\Delta t \qquad\qquad H = I_2 \to \bar{H} = \begin{bmatrix} 1 & 0 \\ 0 & \Delta t^{-1} \end{bmatrix} \tag{42}$$

and the process noise term $\bar{Q} = Q/\Delta t$. Substituting into the Riccati equation and solving for the terms in the covariance matrix yields

$$\begin{aligned}
P_{11} &= \sqrt{2}\sigma_{rx}^{3/2}\sigma_Q^{1/2}\left[\frac{(1+0.5K)^{1/2}}{(1+K)}\right] \\
P_{22} &= \sqrt{2}\sigma_{rx}^{1/2}\sigma_Q^{3/2}\Delta t^2\left[\frac{(1+0.5K)^{1/2}}{(1+K)}\right] \\
P_{12} &= \frac{\sigma_{rx}\sigma_Q\Delta t}{(1+K)} \\
\text{where } K &= \frac{\sigma_Q\sigma_{rx}}{\sigma_{r\dot{x}}^2}
\end{aligned} \tag{43}$$

Substituting Eq. 43 into the Hill's expansion used in Section A yields a matrix equation in the same form as Eq. 25, however, the matrix D is now redefined as

$$D = \begin{bmatrix} \bar{C} & 0_2 \\ 0_2 & \bar{C} \end{bmatrix} \qquad\qquad \bar{C} = \begin{bmatrix} \Delta t/\sigma_{rx}^2 & 0 \\ 0 & 1/(\sigma_{r\dot{x}}^2\Delta t) \end{bmatrix} \tag{44}$$

This set of matrix equations once again indicates that $P_{1_{\mathbf{xx}}} = P_{1_{\mathbf{yy}}} = 0_2$. Solving the system of matrix equations yields

$$P_{1_{\mathbf{xy}}} = P_{1_{\mathbf{x'y'}}} = 0_2 \tag{45}$$

$$P_{1_{\mathbf{xy'}}} = -P_{1_{\mathbf{x'y}}} = -2\frac{\sigma_{rx}^2 P_{0_{\mathbf{xx'}}}}{\Delta t P_{0_{\mathbf{xx}}}}\left(\frac{1}{1+K}\right) \tag{46}$$

Solving for the correlation coefficient, $\rho_{x\dot{y}}$, gives

$$\rho_{x\dot{y}} \approx \frac{\epsilon P_{1_{\mathbf{xy'}}}}{(P_{0_{\mathbf{xx}}}P_{0_{\mathbf{y'y'}}})^{\frac{1}{2}}} \approx -n\sqrt{\frac{\sigma_{rx}}{\sigma_Q}}\left(\frac{1}{1+0.5K}\right) \tag{47}$$

From Eq. 47, it can be seen that as the velocity measurement becomes more accurate (K increases), the correlation magnitude is reduced. This is consistent with the observation that the filter makes more use of dynamics when there are fewer measurements. Substituting this value for $\rho_{x\dot{y}}$ into the expression for semimajor axis standard deviation yields

$$\sigma_{\Delta a} = \frac{2^{\frac{5}{4}}}{n}\sigma_{rx}^{\frac{1}{4}}\sigma_Q^{\frac{3}{4}}\left[\frac{\sigma_Q\sigma_{rx} + 4\sigma_R^2 n^2 + 2\sigma_{r\dot{x}}^2}{\sigma_Q\sigma_{rx} + \sigma_R^2 n^2 + 2\sigma_{r\dot{x}}^2}\right]^{1/2}\left[\frac{(1+0.5K)^{\frac{1}{4}}}{(1+K)^{\frac{1}{2}}}\right]\left[1 + 0.5\left(\frac{n\sigma_{rx}}{\sigma_{r\dot{x}}}\right)^2\frac{1}{1+0.5K}\right]^{\frac{1}{2}} \tag{48}$$

V.   Conclusions

This paper was motivated by the desire to 1) determine what metrics should be used to characterize the filter performance as "good," and 2) explore what parameters in the Kalman filter have the most impact on the performance of the navigation system. Closed loop control performance, which the navigation system exists to support, is dependent on accurate knowledge of the semimajor axis. Analytical work showed that a Kalman filter will not be able to produce the requisite correlation without a process noise level significantly lower than is likely to be possible. Further work showed that the balance and correlation requirements are incompatible. An examination of the effects of velocity measurements demonstrated that such measurements tend to reduce the correlation magnitude, making a $\rho \to -1$ even more difficult to achieve. Increasing the time step of the discrete filter implementation tended to strengthen the correlation, but because the balance property was not simultaneously satisfied, the SMA accuracy also degraded.

Acknowledgments

References

[1] J. Leitner, F. Bauer, D. Folta, M. Moreau, R. Carpenter, J. How, "Distributed Spacecraft Systems Develop New GPS Capabilities," in *GPS World: Formation Flight in Space* Feb. 2002.

[2] F. H. Bauer, J. O. Bristow, J. R. Carpenter, J. L. Garrison, K. Hartman, T. Lee, A. Long, D. Kelbel, V. Lu, J. P. How, F. Busse, P. Axelrad, and M. Moreau, "Enabling Spacecraft Formation Flying through Spaceborne GPS and Enhanced Autonomy Technologies," in *Space Technology*, Vol. 20, No. 4, p. 175–185, 2001.

[3] M. Tillerson, G. Inalhan, and J. How, "Coordination and Control of Distributed Spacecraft Systems Using Convex Optimization Techniques," *Int. Journal of Robust and Nonlinear Control*, vol 12, Issue 2-3, Feb.-Mar. 2002, p.207-242.

[4] J. R. Carpenter and K. T. Alfriend, "Navigation Accuracy Guidelines for Orbital Formation Flying," AIAA G*uidance, Navigation, and Control Confrence*, Austin, TX, Aug 11-4, 2003.

[5] M. Mitchell, L. Breger, J. P. How, and T. Alfriend, "Effects of Navigation Filter Properties on Formation Flying Control," presented at the *AIAA Guidance, Navigation and Control Conference,* Aug. 2004. AIAA-2004-5024

[6] J. R. Carpenter and E. Schiesser, "Semimajor Axis Knowledge and GPS Orbit Determination," in *Journal of the Institute of Navigation* Vol. 48, No. 1, Spring 2001.

[7] J. How and M. Tillerson, "Analysis of the Impact of Sensor Noise on Formation Flying Control," Proceedings of the *American Control Conference*, June 25-27, 2001, p. 3986-3991.

[8] M. Kaplan, *Modern Spacecraft Dynamics and Control*. Wiley, 1976.

[9] A. Gelb, *Applied Optimal Estimation*. MIT Press, 1974.

[10] M. Grewal and A. Andrews, *Kalman Filtering*. Wiley, 2001.

[11] F. Busse, *Precise Formation-State Estimation in Low Earth Orbit Using Carrier Differential GPS,* Ph.D. Dissertation, Stanford University, Dept. Aeronautics and Astronautics, Feb. 2003.

[12] F. D. Busse, J. Simpson, and J. P. How, "Demonstration of Adaptive Extended Kalman Filtering for LEO Formation Estimation Using CDGPS," *Navigation* Journal of the Institute of Navigation, Vol. 50, No. 2, Summer 2003, pp. 79–94.

[13] G. Franklin, J. Powell, M. Workman, *Digital Control of Dynamic Systems,* Second Edition,Addison-Wesley, 1998.

[14] J. Junkins, M. Akella, and K.T. Alfriend, "Non-Gaussian Error Propagation in Orbital Mechanics," in *The Journal of the Astronautical Sciences*, Vol. 44, No. 4, 1996.

[15] M. Mitchell, *CDGPS-Based Relative Navigation for Multiple Spacecraft*, S.M. Thesis, Massachusetts Institute of Technology, Dept. Aeronautics and Astronautics, June 2004.